Astro/Space Seminar, 5 April 2016

MAVEN
CU/LASP • GSFC • UCB/SSL • LM • JPL

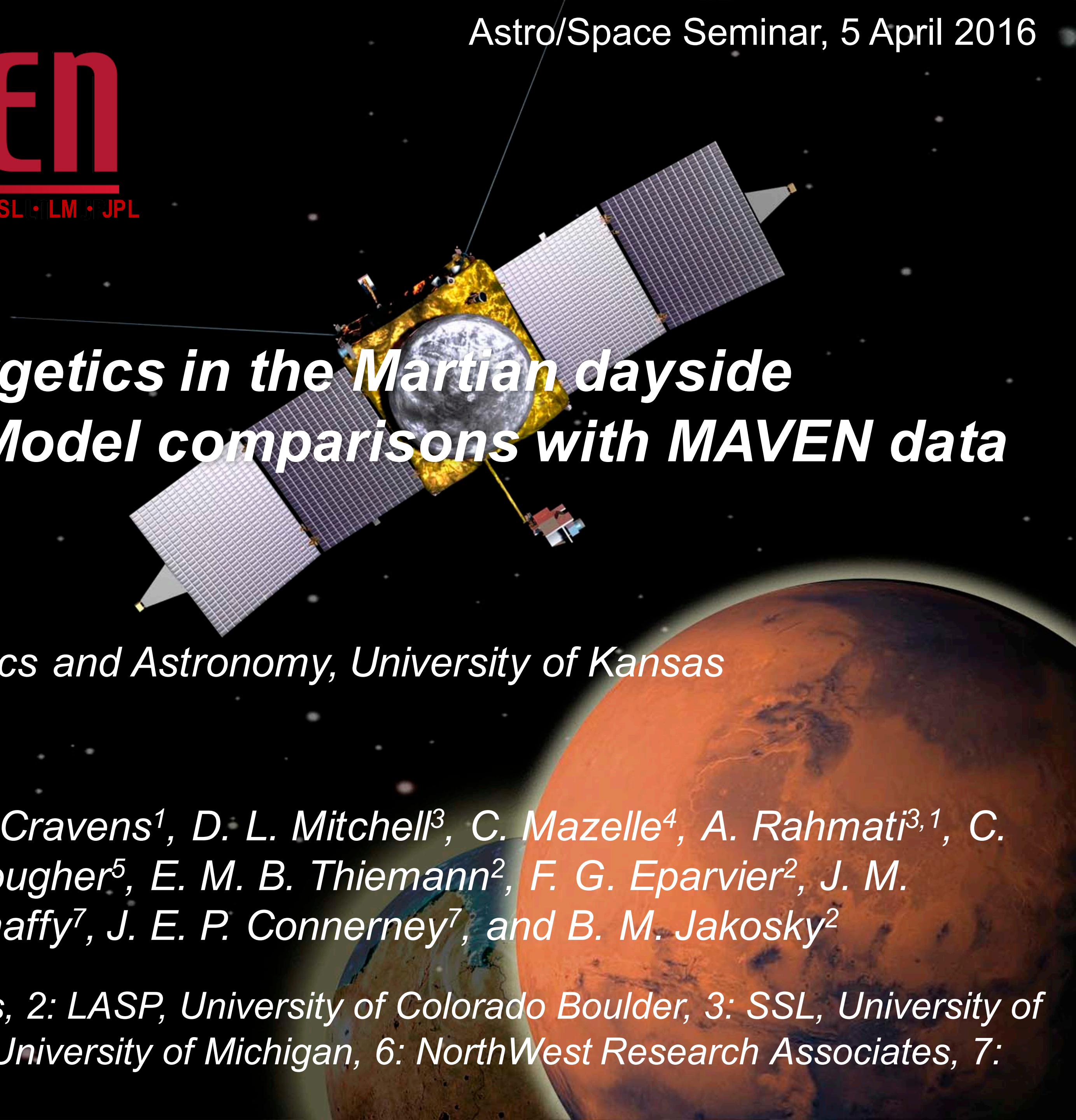

Electron energetics in the Martian dayside ionosphere: Model comparisons with MAVEN data

Shotaro Sakai

Department of Physics and Astronomy, University of Kansas

Collaborators:

L. Andersson[2], T. E. Cravens[1], D. L. Mitchell[3], C. Mazelle[4], A. Rahmati[3,1], C. M. Fowler[2], S. W. Bougher[5], E. M. B. Thiemann[2], F. G. Eparvier[2], J. M. Fontenla[6], P. R. Mahaffy[7], J. E. P. Connerney[7], and B. M. Jakosky[2]

1: University of Kansas, 2: LASP, University of Colorado Boulder, 3: SSL, University of California, 4: IRAP, 5: University of Michigan, 6: NorthWest Research Associates, 7: NASA GSFC

Introduction

- Martian atmospheric escape
  - Thermal escape and non thermal escape
    - Focus on the photochemical escape

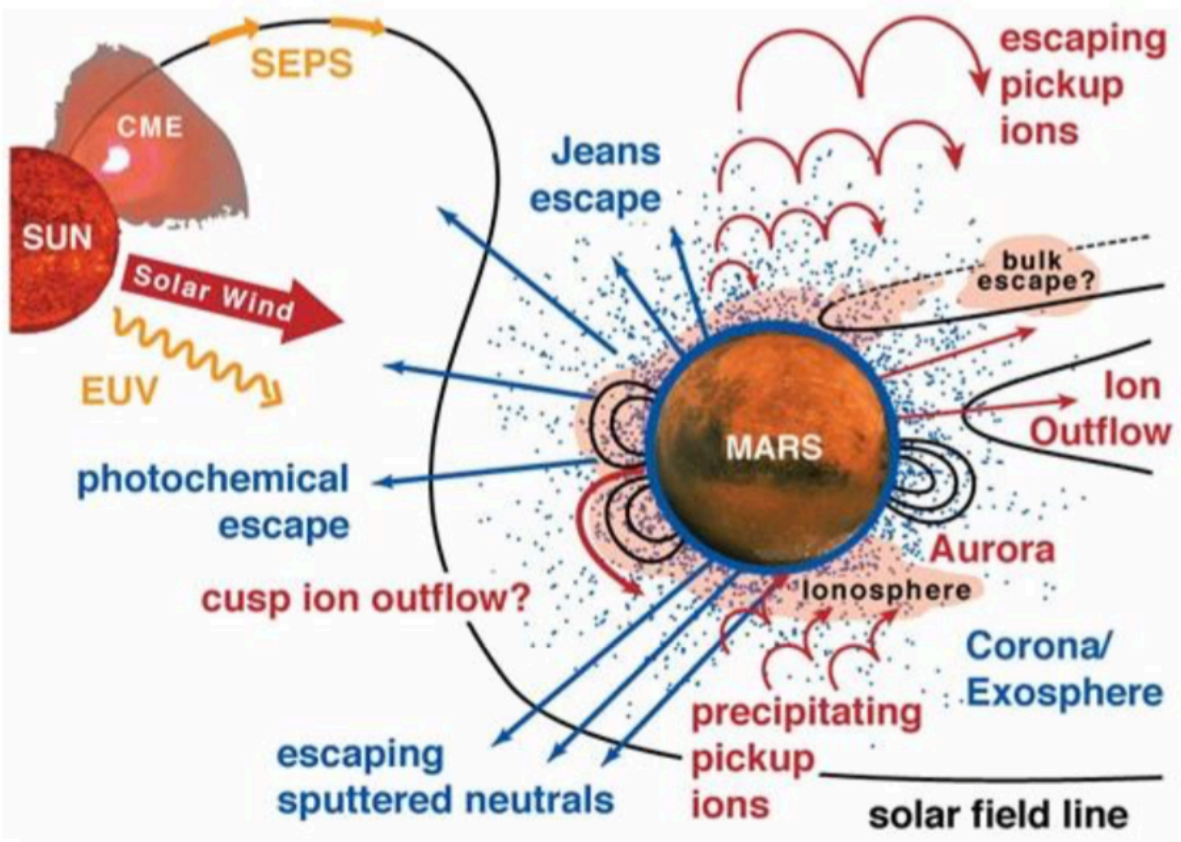

[Courtesy: NASA]

Introduction

- Photochemical escape
  - Key parameter: path of oxygen atom
    - O_2^+ dissociative recombination [e.g., *Nagy and Cravens*, 1988; *Fox and Hać*, 2009]

$O_2^+ + e^- \rightarrow O + O$ (4 energy channels)

$P = 2\alpha n_{O2+} n_{e-}$ [cm^{-3} s^{-1}] (O primary production rate)

$\alpha = 2.4 \times 10^{-7} (300/T_e)^{0.70}$ [cm^3 s^{-1}] (dissociative recombination rate coefficient)

- Thermal electron temperature affects the dissociative recombination rate in the ionosphere.

Introduction

- Electron temperature in the ionosphere
  - Determined due to the balance between heating and cooling.
    - Heating: Energetic photoelectron (collision with suprathermal electron)

      → It is also modeled in this study.
    - Cooling: Collision (e-neutral and e-ion); vibrational, rotational and electronic excitational cooling by neutrals; chemical reaction of O^+ and CO_2^+

Electron temperature is really important in the ionosphere!!

Motivation

- Investigate the electron temperature and also photoelectron distributions in the Martian ionosphere.
  - Dependences on:
    - Magnetic field topology
    - Solar irradiance model
- Model comparison with MAVEN SWEA and LPW

- O_2^+ dissociative recombination: Implication for photochemical escape

MAVEN

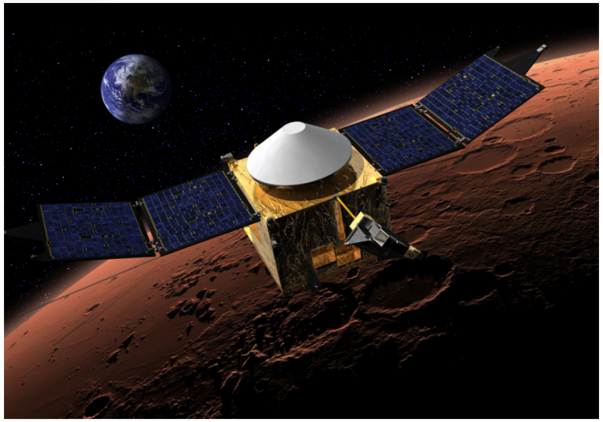

[Courtesy NASA/GSFC]

- Launch: Nov. 18, 2013
- MOI: Sep. 21, 2014
- Orbit
  - Period: 4.5 hrs
  - Periapsis: 150 km (125 km at “deep-dip” campaign)
  - Apoapsis: ~6000 km

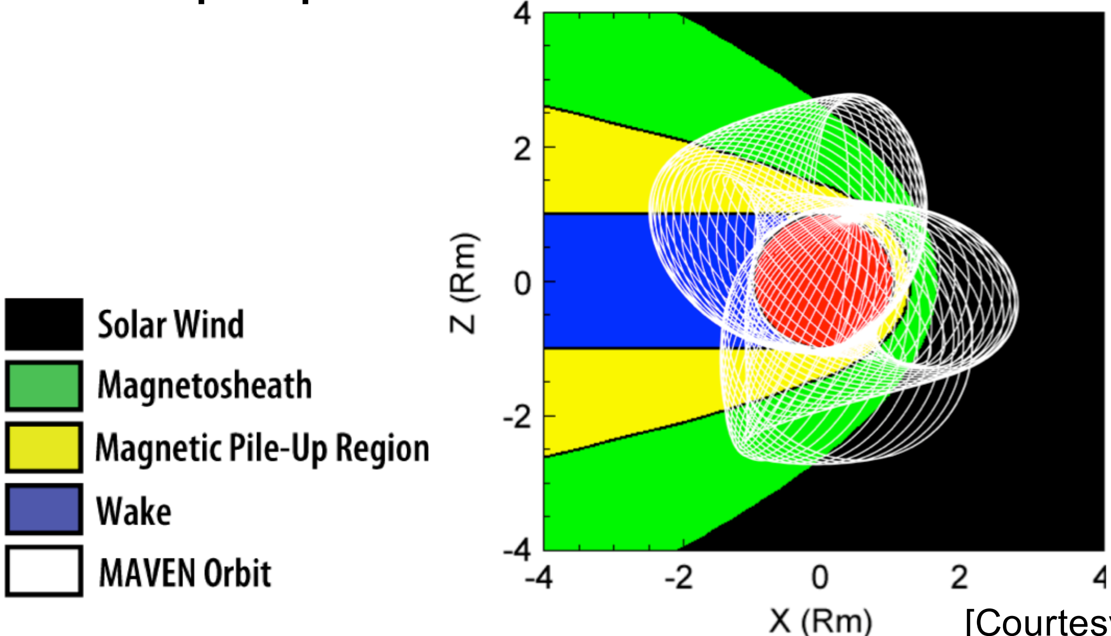

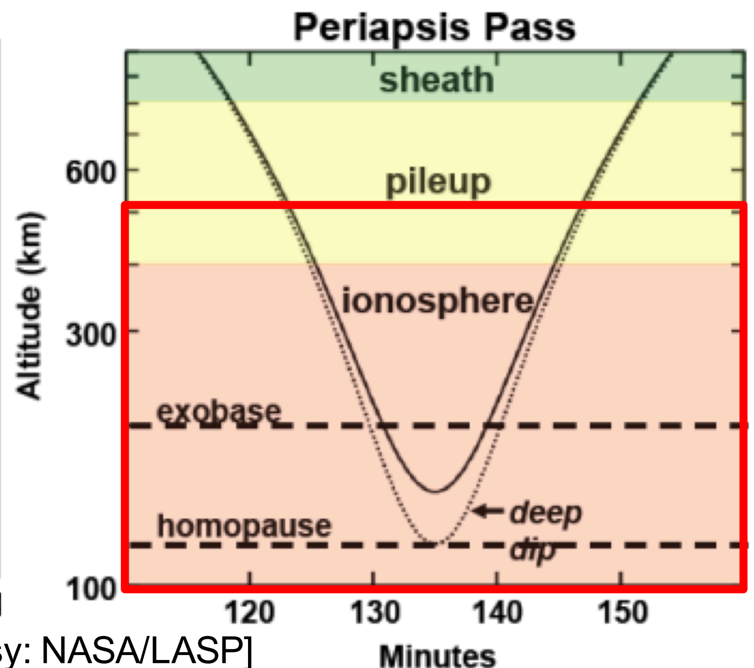

[Courtesy: NASA/LASP]

MAVEN

- Mars Atmosphere and Volatile Evolution Mission (MAVEN)
  - Goal
    - Determining of the role that loss of atmospheric gas to space played in changing the Martian climate through time.
      - Where did the atmosphere and water go from Mars?
  - How much of the Martian atmosphere has been lost over time?
    - Measuring the current rate of escape to space.
    - Gathering enough information about the relevant processes to allow extrapolation backward in time.

MAVEN

- Instruments
  - Solar Wind Electron Analyzer (SWEA)
  - Solar Wind Ion Analyzer (SWIA)
  - Suprathermal and Thermal Ion Composition (STATIC)
  - Solar Energetic Particle (SEP)
  - Langmuir Probe and Waves (LPW)
  - Extreme Ultraviolet Monitor (EUVM)
  - Magnetometer (MAG)
  - Imaging Ultraviolet Spectrograph (IUVS)
  - Neutral Gas and Ion Mass Spectrometer (NGIMS)

In-situ observations before MAVEN

- Only two Viking landers observed the electron temperature in the ionosphere [*Hanson and Mantas*, 1988].

- Three electron populations
  - $T_{e1} \approx 3000$ K
    - Thermal electrons
  - $T_{e2} \approx 30000$ K
    - Photoelectrons
  - $T_{e3} \approx 200000$ K
    - Electrons of solar wind origin

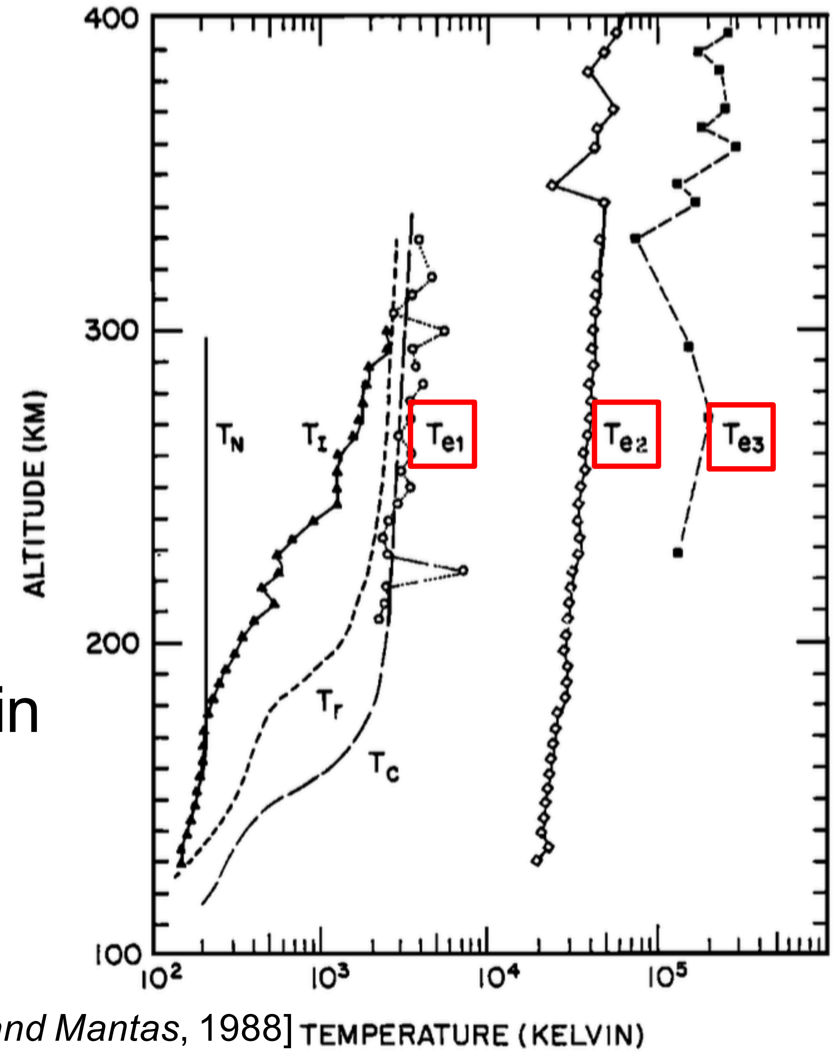

Electron temperatures measured by Viking [*Hanson and Mantas*, 1988]

Models before MAVEN

- Several models were successful in reproducing the Te of Viking observations [*Chen*+, 1978; *Johnson*, 1978; *Rohrbaugh*+, 1979; *Singhal and Whitten*, 1988; *Choi*+, 1998; *Matta*+, 2014].

Recent work [*Matta*+, 2014]

- Model required topside heat fluxes of
  - e^- Flux: 1.5×10^{10} [eV cm^{-2} s^{-1}]
  - Ion Flux: 2×10^{7} [eV cm^{-2} s^{-1}]

to match the Viking observations.

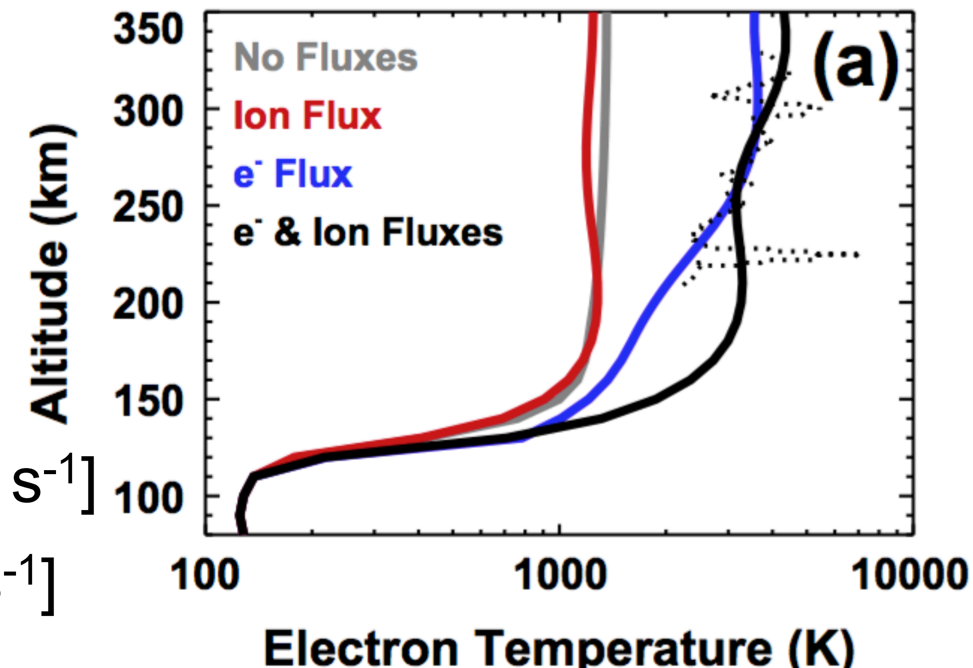

Electron temperatures [*Matta*+, 2014]

MAVEN observations

- Langmuir Probe: Orbits 819, 873 and 337

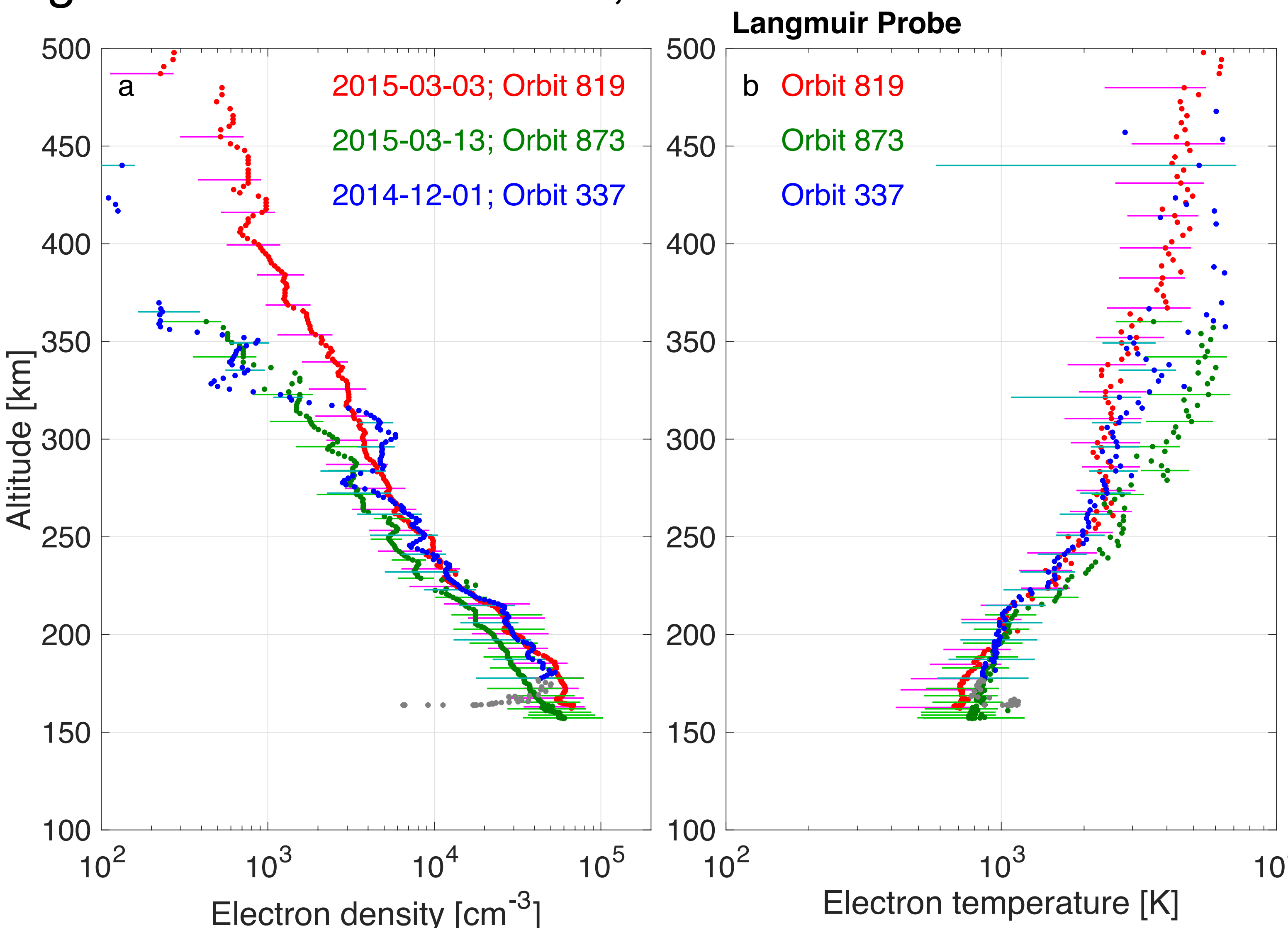

Electron densities and temperature from MAVEN/LPW [*Sakai*+, submitted]

Selection of orbits

- Orbits 819 (03/03/15), 873 (03/13/15) and 337 (12/01/14)
- Criteria
  - Magnetic dip angle ≈ 0˚ (almost solar wind condition)
    - Avoided the crustal magnetic field from the surface.
    - Mars does not have intrinsic magnetic fields such as the Earth's.
  - Insignificant solar flare
  - Dayside

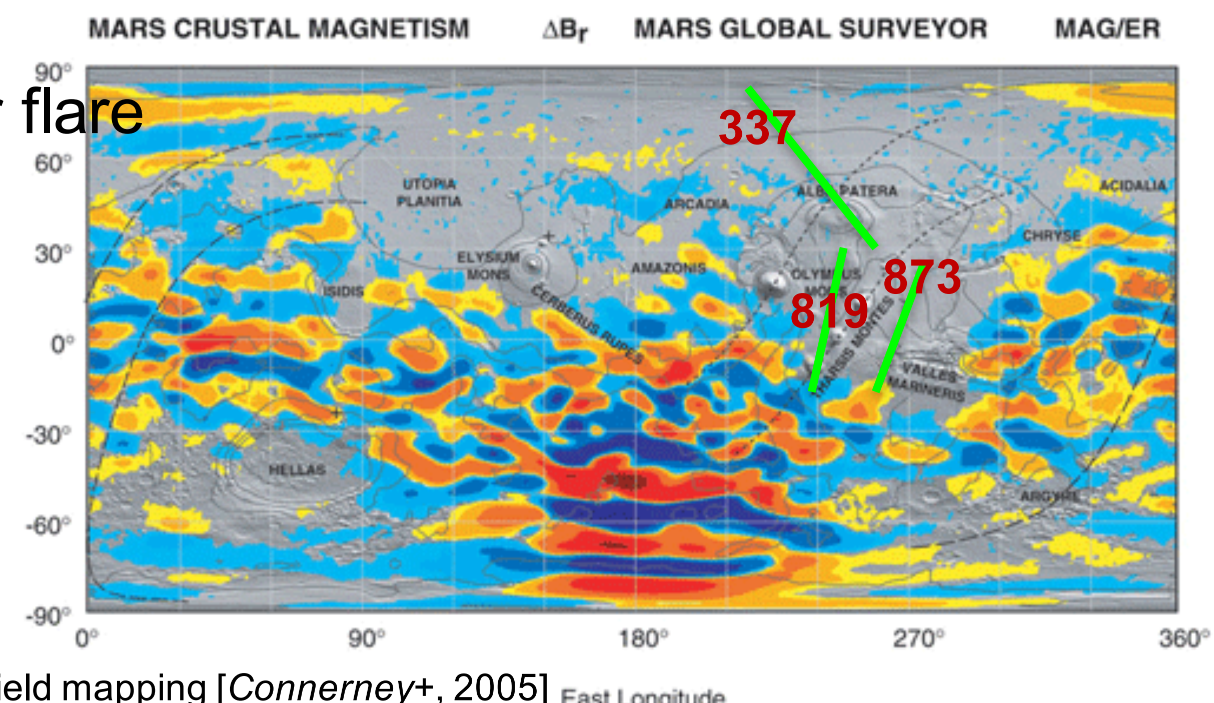

Crustal magnetic field mapping [*Connerney*+, 2005]

Model

Solar irradiance model

- Input solar irradiances
  - Test 2 cases
    1. HESSR
       - Based on the Solar Irradiance Physical Modeling system [e.g., *Fontenla*+, 2011]
    2. FISM-M
       - Based on the MAVEN EUV monitor [*Eparvier*+, 2015]

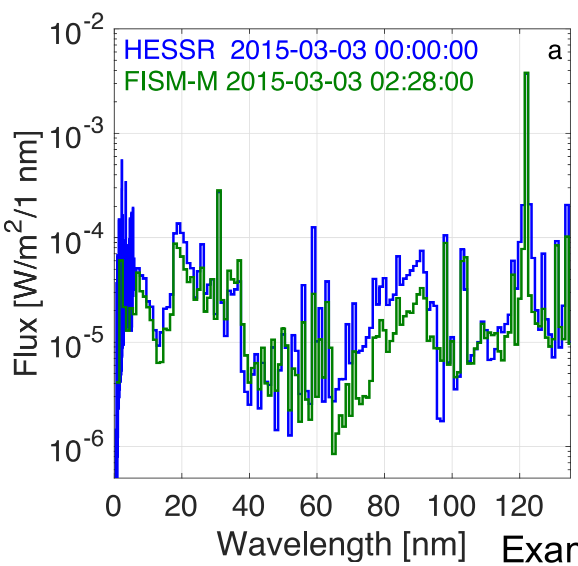

Example of solar irradiance [*Sakai*+, submitted]

Photoelectron heating rate

- Two-stream photoelectron transport code [e.g., *Sakai*+, 2015]
  - Calculates up-flow and down-flow energy flux of photoelectrons (heating rate in ionosphere)

$$\langle \mu \rangle \frac{d\Phi^{\pm}}{ds} = -\sum_k n_k(s)\left(\sigma_a^k + p_s^k \sigma_s^k\right)\Phi^{\pm}(\varepsilon, s) + \sum_k n_k(s)\, p_e^k \sigma_e^k \Phi^{\mp}(\varepsilon, s) + \frac{q(\varepsilon, s)}{2} + q^{\pm}(\varepsilon, s)$$

- Background atmosphere
  - Fitted to NGIMS from MTGCM
    - NGIMS (Neutral Gas and Ion Mass Spectrometer onboard MAVEN)
    - MTGCM (Mars Thermospheric General Circulation Model [e.g., *Bougher*, 2012])

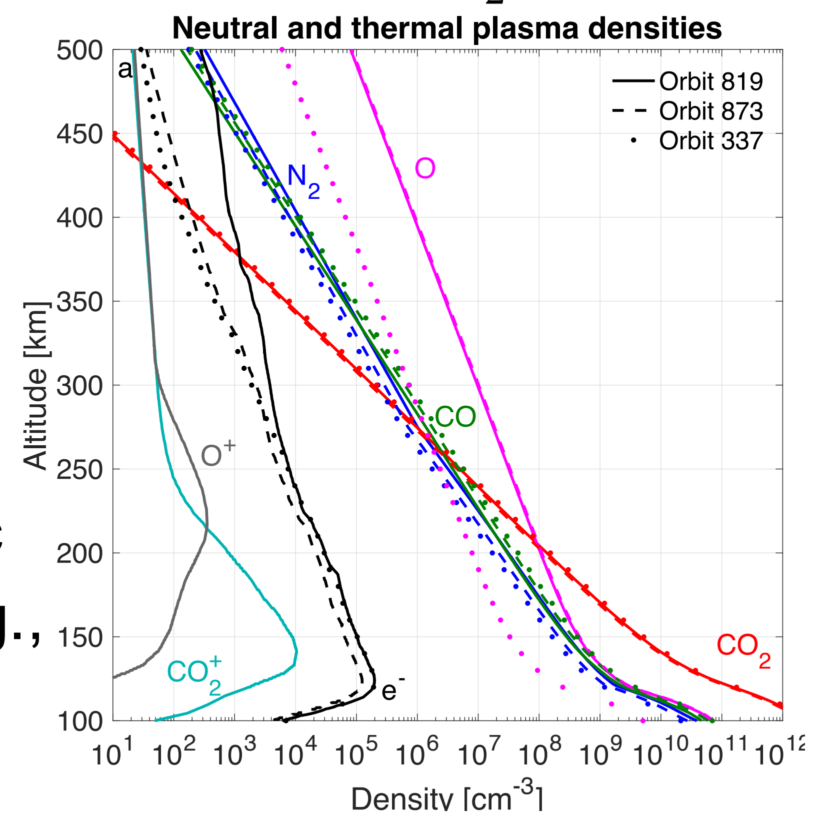

Neutral & plasma densities [*Sakai*+, submitted]

Electron temperature

- Energy equation

$$\frac{3}{2}n_s k_B \frac{\partial T_s}{\partial t} + \frac{3}{2}n_s k_B \mathbf{u}_s \cdot \nabla T_s + \frac{3}{2}n_s k_B T_s \nabla \cdot \mathbf{u}_s + \frac{3}{2}\left(T_s - T_n\right) S_s + \nabla \cdot \left(-K_s \nabla T_s\right)$$

$$= \sum_t \frac{n_s m_s \nu_{st}}{m_s + m_t}\left[3k_B\left(T_t - T_s\right) + m_t\left(\mathbf{u}_s - \mathbf{u}_t\right)^2\right] + Q_s - L_s$$

- Background atmosphere
  - Neutral temperature from MTGCM

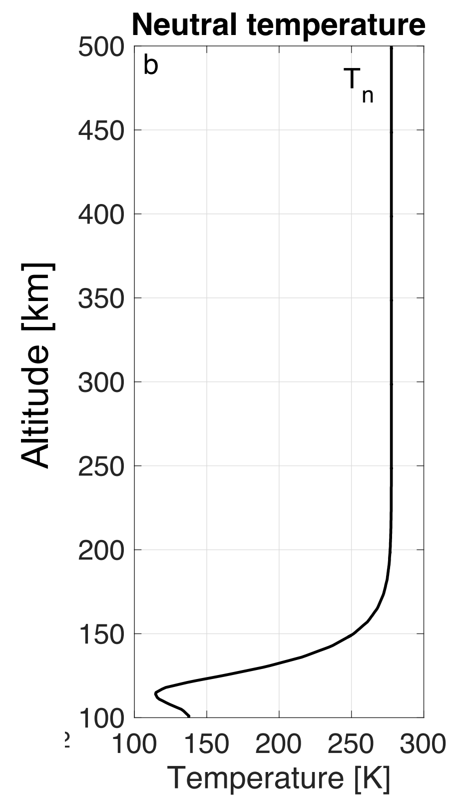

Neutral temperature [*Sakai*+, submitted]

Magnetic topology

- It is complex because solar wind-induced magnetic fields and local crustal magnetic fields are both present [*Acuña*+, 1998].
- Categorized as four general types
  1. Draped/induced fields that are open to the solar wind and/or magnetotail at both ends (solar wind origin)
  2. Draped, largely horizontal fields, open at one end to the solar wind and/or magnetotail and attached to Mars at the other end (solar wind origin)
  3. Crustal fields that are closed at both ends and are attached to the planet (crustal field origin)
  4. Crustal fields closed at one end and open to the solar wind or tail at the other end and with significant radial components (crustal field origin)

Magnetic topology

- It is complex because solar wind-induced magnetic fields and local crustal magnetic fields are both present [*Acuña*+, 1998].
- Categorized as four general types
  1. Draped/induced fields that are open to the solar wind and/or magnetotail at both ends (solar wind origin)
  2. Draped, largely horizontal fields, open at one end to the solar wind and/or magnetotail and attached to Mars at the other end (solar wind origin)
  3. Crustal fields that are closed at both ends and are attached to the planet (crustal field origin)
  4. Crustal fields closed at one end and open to the solar wind or tail at the other end and with significant radial components (crustal field origin)

Coordinate

1. Draped/induced fields that are open to the solar wind and/or magnetotail at both ends (nested draped field lines)

a: Multiple field lines

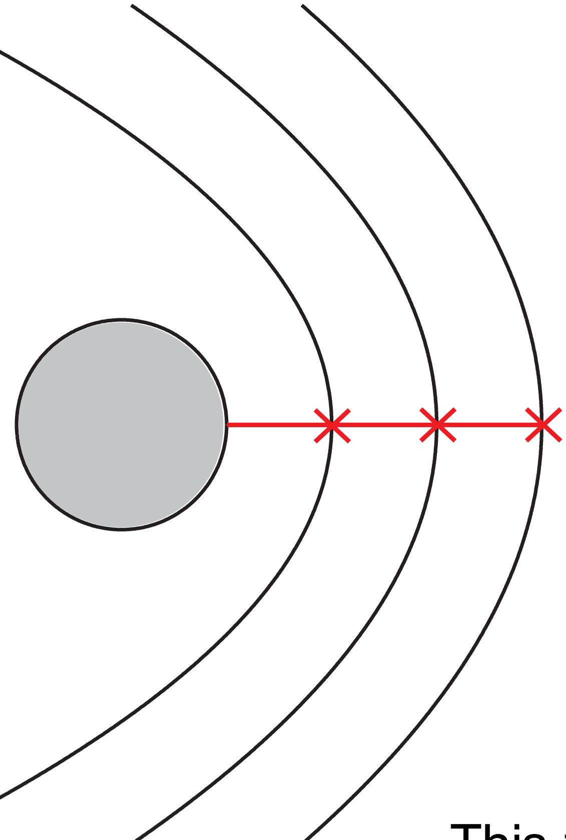

This figure is not to scale.

[*Sakai*+, submitted]

Results: Comparison with SWEA

- Photoelectron fluxes for Orbits 819 and 873
  - Below 250 km: Model agree with SWEA within a factor of 2.5.
    - 200 km in low E: N_e/N_n is important [*Sakai*+, 2015].
  - Above 300 km: Tail electron and solar wind affect the fluxes above 70 eV.

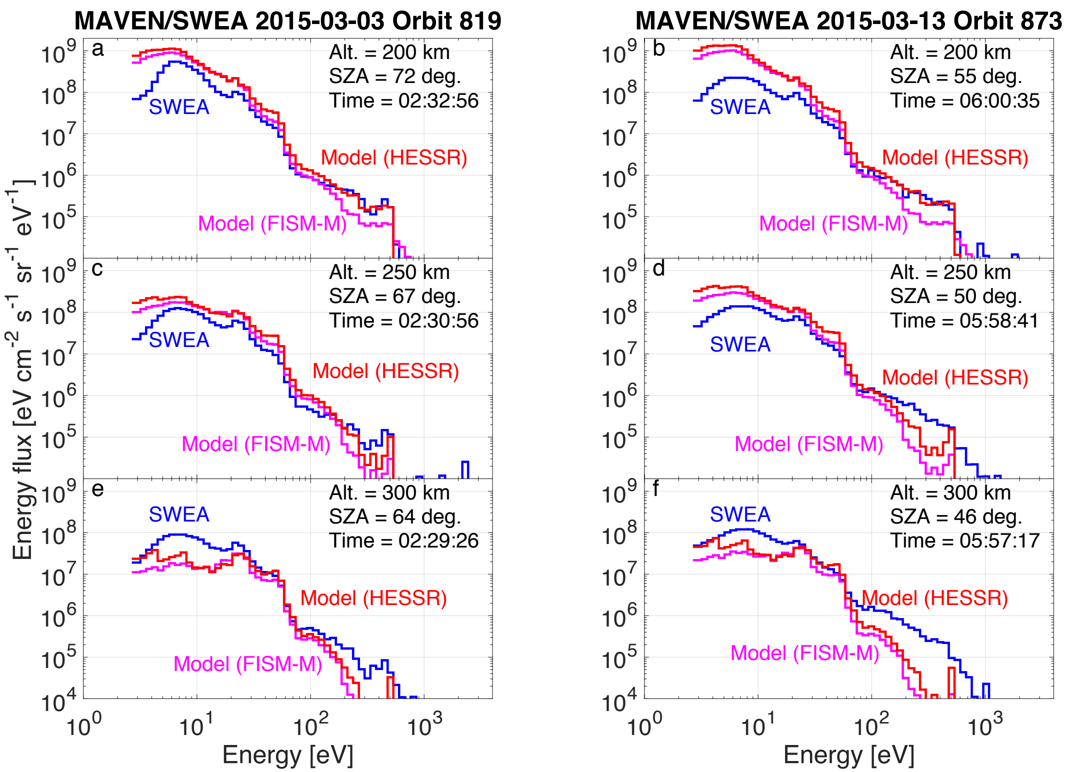

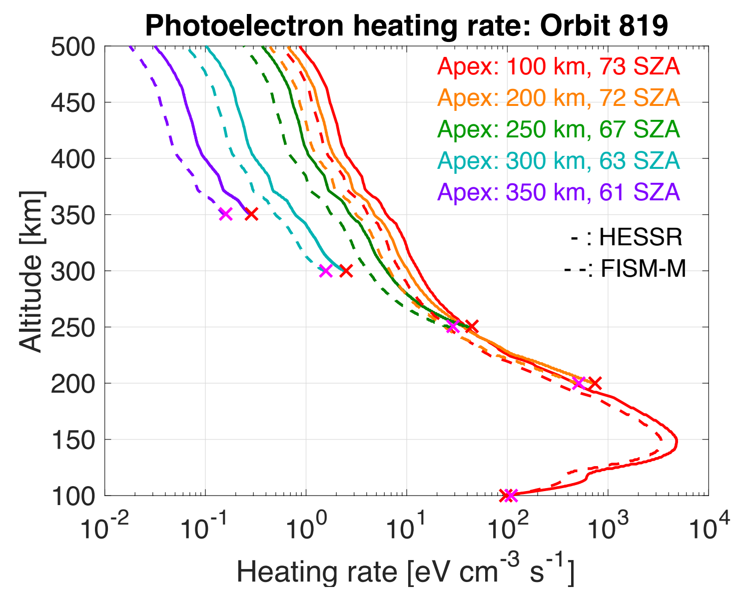

Model and SWEA photoelectron fluxes, and heating rate [*Sakai*+, submitted]

Results: Comparison with SWEA

- Flux with HESSR (red) > Flux with FISM-M (magenta)
  - HESSR irradiance is higher than FISM-M.
- Heating rate
  - Peak heating rate around altitude of the maximum density
  - Decreases with increasing altitude.

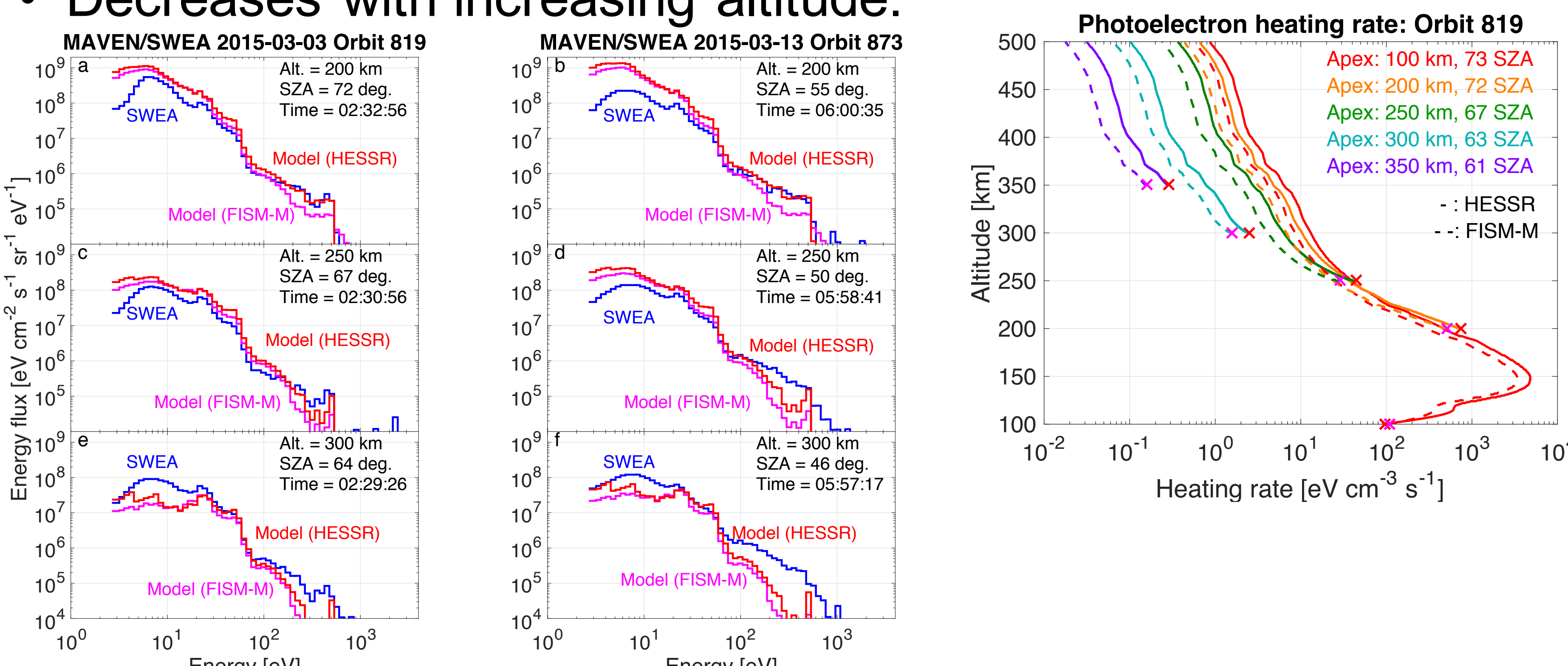

Model and SWEA photoelectron fluxes, and heating rate [*Sakai*+, submitted]

Results: Comparison with LPW

- Electron temperatures for Orbits 819 and 873
  - Models agree with LPW observations above 250 km.
    - Te with HESSR is higher than that of FISM-M.
  - Successful on obtaining high electron temperatures without invoking topside heat fluxes.

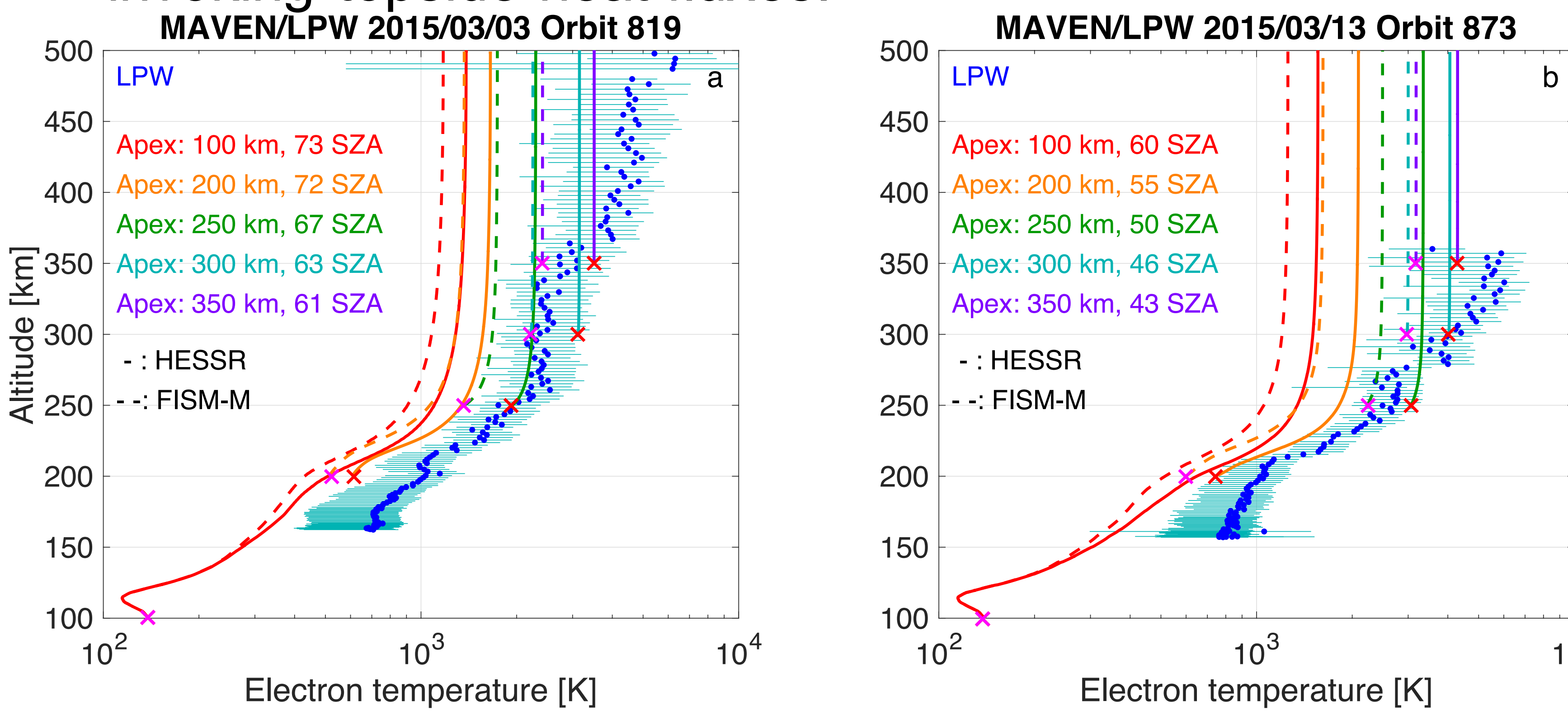

Model and LPW electron temperatures [*Sakai*+, submitted]

Results: Comparison with SWEA

- Photoelectron fluxes for Orbit 337

Nested draped field lines

- Models does not agree with SWEA observations above 250 km.

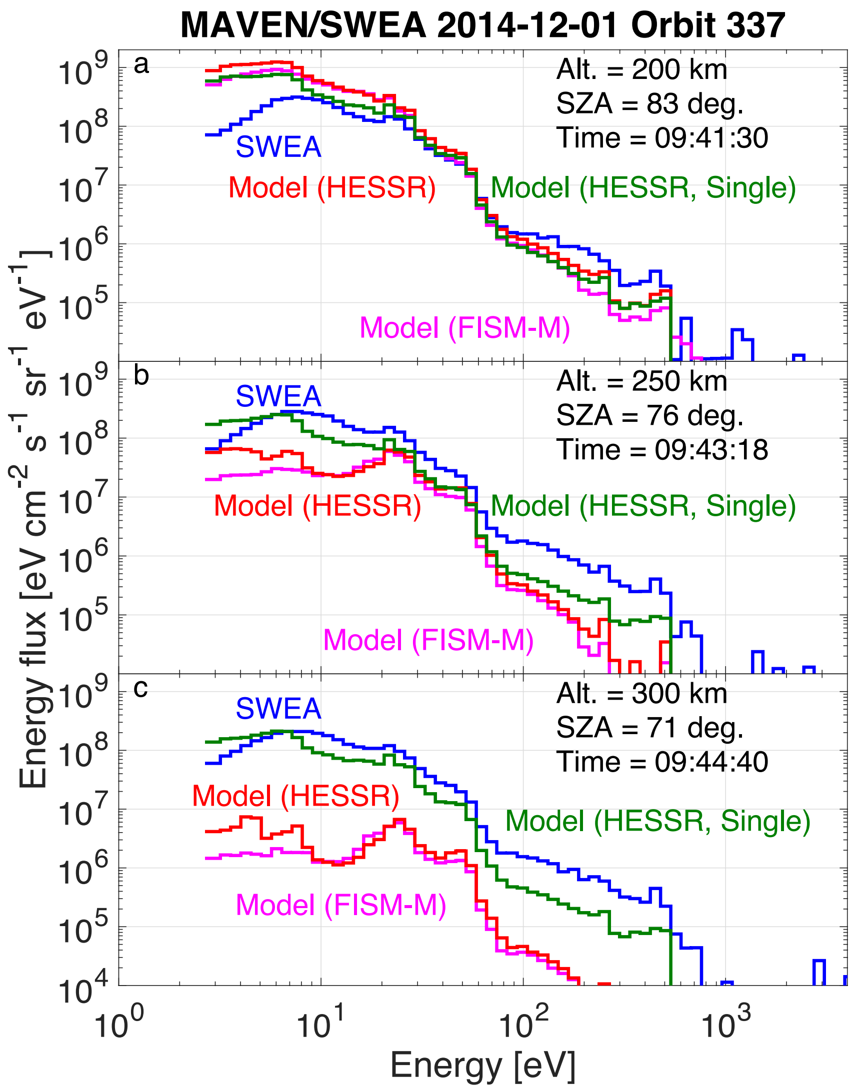

Model and SWEA photoelectron fluxes for Orbit 337 [*Sakai*+, submitted]

Coordinate

2. Draped, largely horizontal fields, open at one end to the solar wind and/or magnetotail and attached to Mars at the other end

b: Single field line

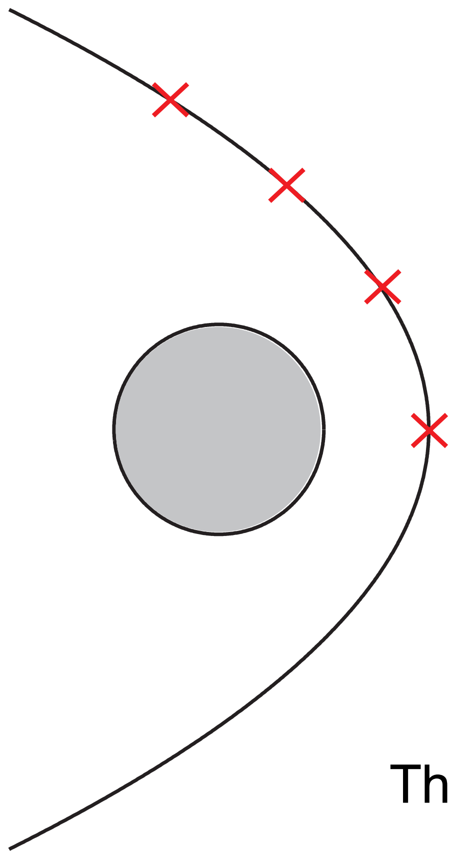

This figure is not to scale.

[*Sakai*+, submitted]

Results: Comparison with SWEA

- Photoelectron fluxes for Orbit 337

Single field line

- Models agree with SWEA below 70 eV
  - Transport from low altitude is important.
- Tail electrons or solar wind are related to fluxes above 70 eV.

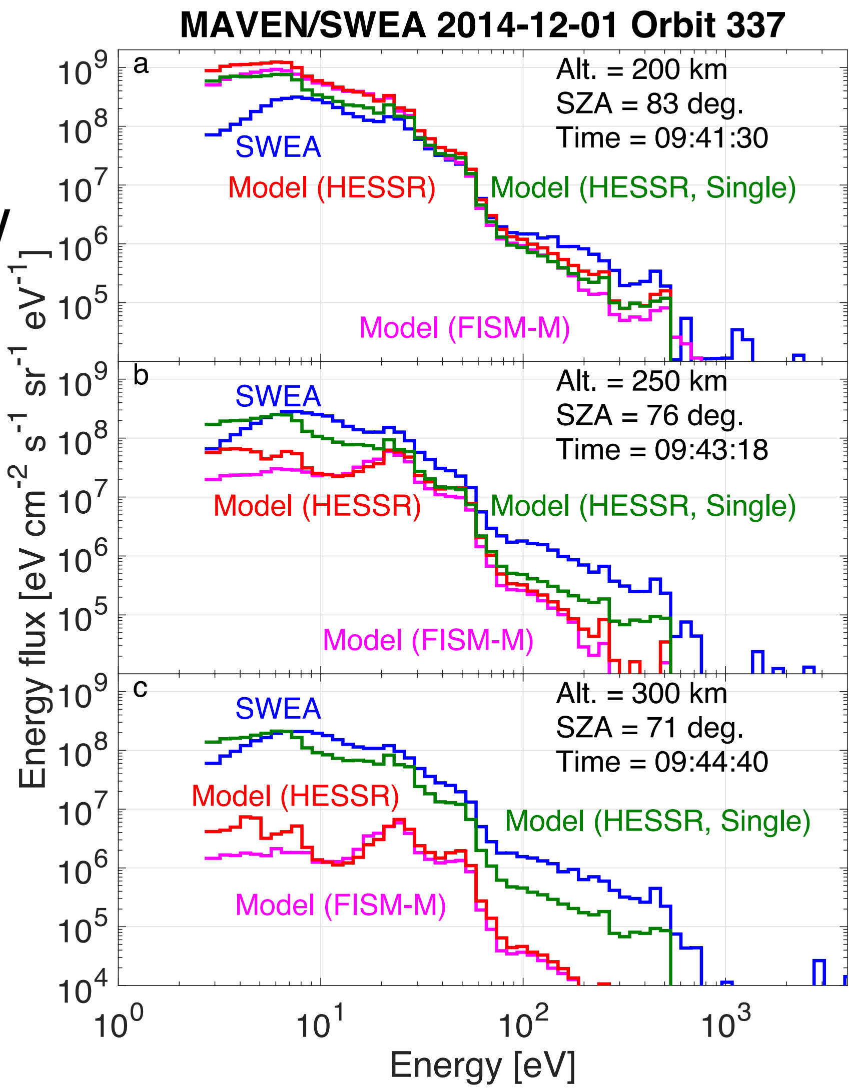

Model and SWEA photoelectron fluxes for Orbit 337 [*Sakai*+, submitted]

Results: Comparison with LPW

- Electron temperature for Orbit 337

Single field line (black)

- Model is lower than LPW.
  - Tail electron could be a heat source of thermal electrons

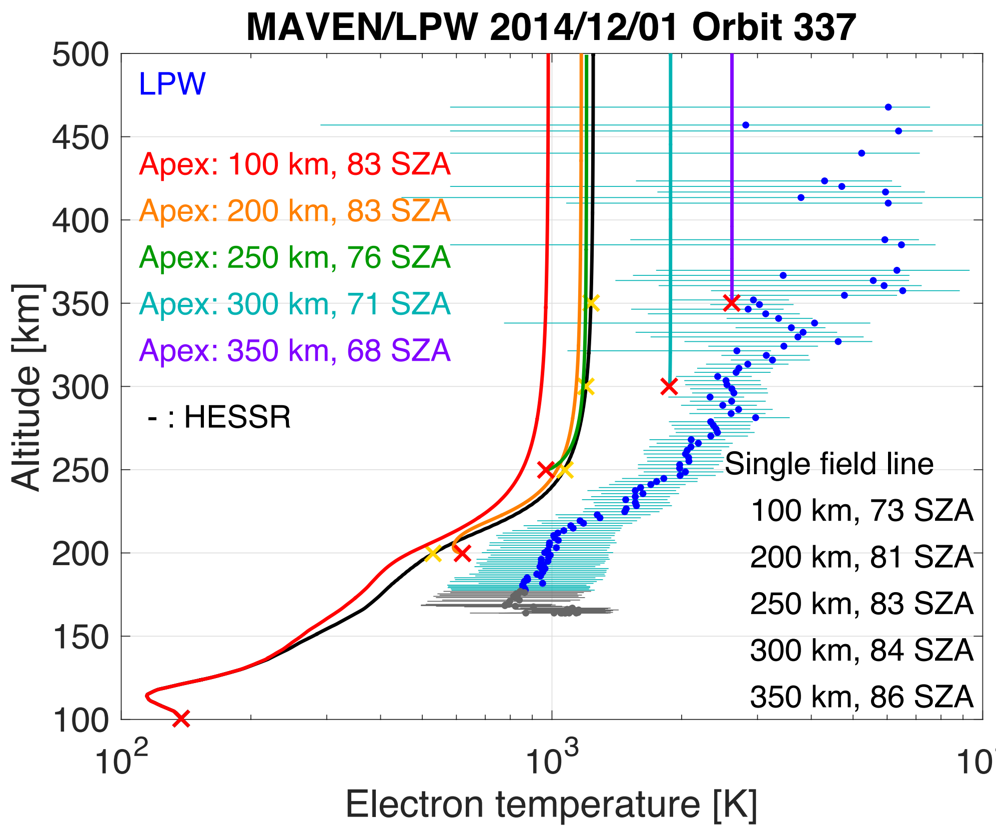

Model and LPW electron temperatures for Orbit 337 [*Sakai*+, submitted]

Dissociative recombination

- O_2^+ dissociative recombination for Orbits 819 and 873
- DR rate coefficient
  - $\alpha = 2 \times 10^{-7}$ [$cm^3\ s^{-1}$] at 150 km
  - $\alpha = 1.3 \times 10^{-7}$ [$cm^3\ s^{-1}$] near the exobase
  - Differences between model and observations are about 30 – 100%.
    - It will affect ionospheric density calculations and hot oxygen atom production rate.

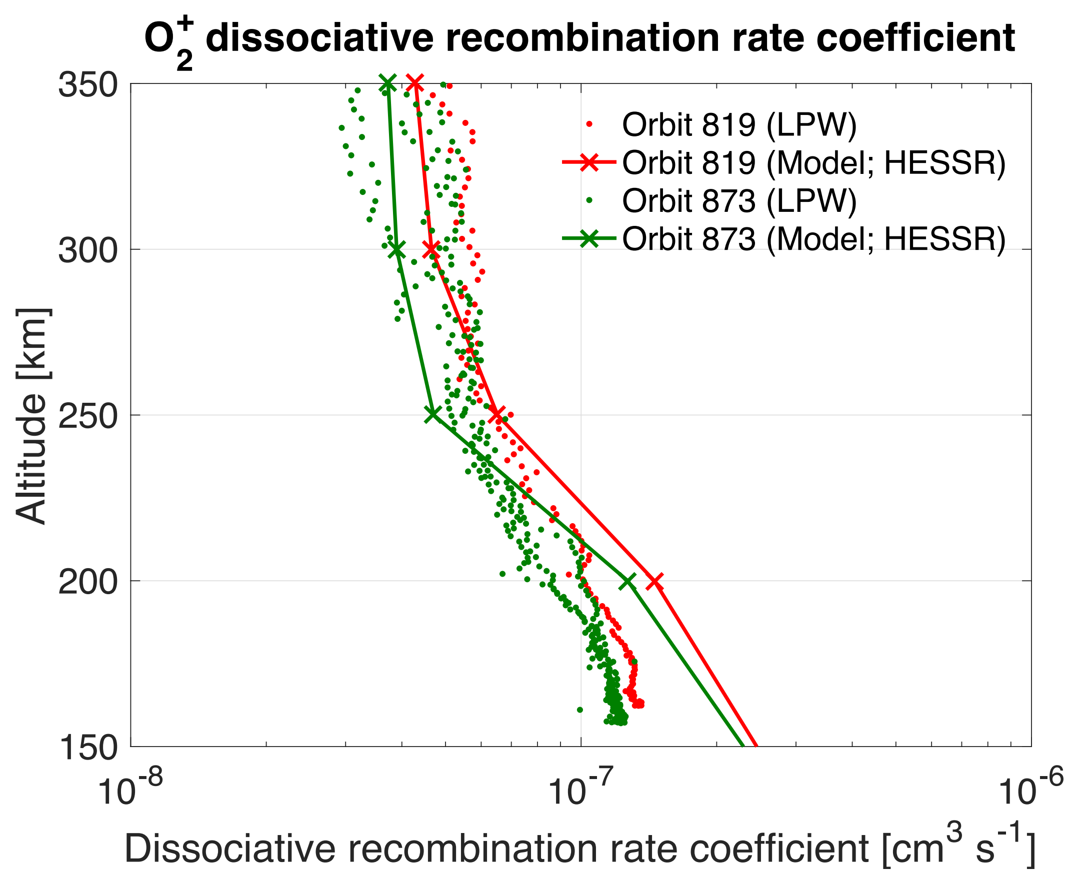

O_2^+ DR rate coefficients [*Sakai*+, submitted]

Summary

- Investigated the photoelectron fluxes and thermal electron temperatures in the Martian upper atmosphere.
- Successful on producing high electron temperatures at high altitudes without invoking heat fluxes from the top.
- The topology and position of magnetic field lines are important factors in determining the profile of T_e and photoelectron distribution.
  - Orbits 819 and 873: Draped nested fields
  - Orbit 337: Single field line; Transport from low altitude
- O_2^+ DR rate coefficients differences between model and LPW are about 30 – 100 %.
  - This difference will affect ionospheric density calculations and hot oxygen atom production rates.

References

- Acuña, m. H., et al. (1998), Magnetic field and plasma observations at Mars: Initial results of the Mars Global Surveyor mission, Science, 279, 1676-1680.
- Bougher, S. W. (2012), Coupled MGCM-MTGCM Mars thermosphere simulations and resulting data products in support of the MAVEN mission, *JPL/CDP report*, pp. 1-9, 6 August.
- Chen, R. H., T. E. Cravens, and A. F. Nagy (1978), The Martian ionosphere in light of the Viking observations, J. Geophys. Res., 83, 3871-3876.
- Choi, Y. W., J. Kim, K. W. Min, A. F. Nagy, and K. I. Oyama (1998), Effect of the magnetic field on the energetics of Mars ionosphere, Geophys. Res. Lett., 25, 2753-2756.
- Connerney, J. E. P., M. H. Acuña, N. F. Ness, G. Kletetschka, D. L. Mitchell, R. P. Lin, and H. Reme (2005), Tectonic implications of Mars crustal magnetism, Proc. Nati. Acad. Sci. USA, 102, 42, 14970-14975.
- Fontenla, J. M., J. Harder, W. Livingston, M. Snow, and T. Woods (2011), High-resolution solar spectral irradiance from extreme ultraviolet to far infrared, J. Geophys. Res., 116, D20108.
- Fox, J. L., and A. B. Hac (2009), Photochemical escape of oxygen from Mars: A comparison of the exobase approximation to a Monte Carlo method, Icarus, 204, 527-544.
- Hanson, W. B., and G. P. Mantas (1988), Viking electron temperature measurements: Evidence of a magnetic field in the martian ionosphere, J. Geophys. Res., 93, 7538-7544.
- Johnson, R. E. (1978), Comment on ion and electron temperatures in the martian upper atmosphere, Geophys. Res. Lett., 5, 989-992.
- Nagy, A. F., and T. E. Cravens (1988), Photoelectron fluxes in the ionosphere, J. Geophys. Res., 75, 6260-6270.
- Matta, M., M. Galand, L. Moore, M. Mendillo, and P. Withers (2014), Numerical simulations of ion and electron temperatures in the ionosphere of Mars: Multiple ions and diurnal variations, *Icarus*, 227, 78-88.

References

- Rohrbaugh, R. P., J. S. Nisbet, E. Bleuler, and J. R. Herman (1979), The effect of energetically produced O_2^+ on the ion temperatures of the martian thermosphere, J. Geophys. Res., 84, 3327-3338.
- Sakai, S., A. Rahmati, D. L. Mitchell, T. E. Cravens, S. W. Bougher, C. Mazelle, W. K. Peterson, F. G. Epavier, J. M. Fontenla, and B. M. Jakosky (2015), Model insights into energetic photoelectrons measured at Mars by MAVEN, *Geophys. Res. Lett.*, 42, 8894-8900.
- Sakai, S., L. Andersson, T. E. Cravens, D. L. Mitchell, C. Mazelle, A. Rahmati, C. M. Fowler, S. W. Bougher, F. G. Eparvier, E. M. B. Thiemann, J. M. Fontenla, P. R. Mahaffy, J. E. P. Connerney, and B. M. Jakosky (2016), Electron energetics in the Martian dayside ionosphere: Model comparisons with MAVEN data, *J. Geophys. Res. Space Physics*, submitted.
- Singhal, R. P., and R. C. Whitten (1988), Thermal structure of the ionosphere of Mars: Simulations with one- and two-dimensional models, Icarus, 74, 357-364.